Luminescence properties of Bi^{3+} in Y_2O_3

R M Jafer[1,2] , A Yousif [1,2], E Coetsee[1] and HC Swart[1]

[1] Department of Physics, University of the Free State, P.O. Box 339, Bloemfontein, ZA 9300, South Africa.

[2]Department of Physics, Faculty of Education, University of Khartoum, P.O. Box 321, Postal Code 11115, Omdurman, Sudan.

Corresponding Author Email address: coetseeE@ufs.ac.za

Abstract. The luminescent properties of $Y_{2-x}O_3:Bi_{x=0.002}$ were investigated and the fluorescence spectra show that the luminescence was produced by the emission from two types of centers. These two types of centers were associated with the substitution of the Y^{3+} ion with the Bi^{3+} ion in two different sites in the crystal lattice of Y_2O_3 (with point symmetries C_2 and S_6). The emission of Bi^{3+} in the S_6 site caused blue luminescence with maxima at 360 nm and 407 nm, and in the C_2 site it gave green luminescence with the maximaum at 495 nm. Both these emissions are related to the $^3P_1$-$^1S_0$ transition in Bi^{3+}. The diffuse reflectance was measured for Y_2O_3 and Y_2O_3:Bi. No change in the band gap, when 0.2 mol% of Bi was doped in the Y_2O_3 host, was observed.

1. Introduction

Metal ions with outer ns^2 configuration are of great importance in the luminescence field. The luminescence of Bi^{3+} in oxides, phosphates, aluminates, and borates [1, 2] has been extensively studied since 1960. The Bi^{3+} ion with a $6s^2$ electronic configuration shows strong optical absorption in the near ultraviolet region (300 - 400 nm) due to the s^2-sp transition [3,4]. The $6s^2$ electronic configuration splits into one level for the ground state (singlet $^1S_0$) and four levels for the excited 6s6p state (triplet ($^3P_0$, $^3P_1$ and $^3P_2$) and singlet ($^1P_1$)). The transitions from $^1S_0$ to $^3P_0$ and $^3P_2$ are strongly forbidden due to the Δj selection rule, while the transitions from $^1S_0$ to $^3P_1$ and $^1P_1$ are allowed due to the $^3P_1$ and $^1P_1$ spin – orbital coupling [5,7,11]. In this research we only consider the transition $^1S_0 \rightarrow {}^3P_1$, due to absorption occurring in the range of 300 - 400 nm for the Bi^{3+} ion while the transition $^1S_0 \rightarrow {}^1P_1$ usually is located at higher energies [1,4,11]. Furthermore, it is well known that the level $^3P_1$ split into sublevels due to the crystal field effect, corresponding to the position of the Bi^{3+} in the host [5,8,9].

Y_2O_3 is known as an excellent phosphor material and it is widely used in high-temperature-resistant windows, lighting and display applications, host materials for solid state lasers or scintillators etc. [18]. The crystallographic structure of Y_2O_3 has a C-type cubic structure with each unit cell containing 32 cationic sites. Eight are centrosymmetric with a S_6 symmetry and 24 are non centrosymmetric with a C_2 symmetry [7,11,12]. These two sites have an impact on the excitation and emission spectra of the Y_2O_3 phosphor material [12,19].

In this study the Y_2O_3:Bi phosphor was synthesized by the combustion method and characterized by X-ray diffraction (XRD), photoluminescence (PL) and UV-Vis spectroscopy. PL and UV-Vis spectroscopy were also used to obtain the luminescent mechanism.

2. Experimental

Powder samples of $Y_{2-X}O_3$: $Bi^{3+}{}_{X=0.002}$ were prepared by urea-nitrate solution combustion synthesis. $Y(NO_3)_3.4H_2O$, CH_4N_2O and $Bi(NO_3)_3.5H_2O$ were used as the starting materials, which dissolved in diluted water under stirring and heating to obtain a mixed aqueous homogenous precursor solution. The solution was placed in a furnace preheated at 550^o C. After the combustion process was completed, the obtained solid precursors were then ground and fired at 700 ^{o}C for 1 h in air to produce the final samples. The crystal structure was determined by using a Bruker D8 diffractometer, the

diffuse reflectance spectra were recorded using a Lambda 950 UV-Vis spectrophotometer, PL was measured with a Cary eclipse spectrophotometer and the 325 nm He-Cd laser PL system.

3. Results and discussion

3.1 Structural analysis

The XRD results for the Y_2O_3:Bi powder and the profile of the ICSD reference data file are shown in Figure 1. The results indicated that the single phase cubic crystal structure with Ia-3 space group was formed [10], which is in agreement with the ICSD reference data file no. 16394. The main peak of the cubic structure corresponds well with that for the {222} crystalline plane centred at 29.16°.

In this structure every unit cell has 32 cationic sites with a coordination number of 6. These sites can be substituted by rare earth ions where eight will have the S_6 symmetry and the other 24 will have the C_2 symmetry. The sites with S_6 symmetry are where two oxygen vacancies are located on a cube and the sites with C_2 symmetry are where the vacancies are located on a face diagonal, see Figure 2(a) and (b) [7,11,12].

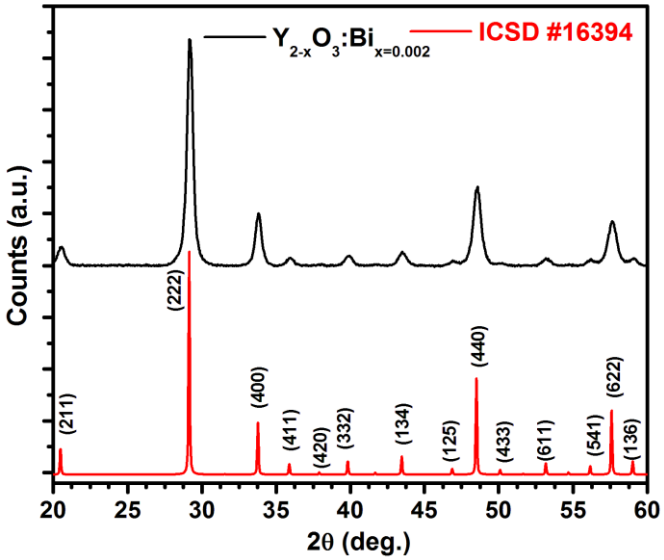

Figure 1: XRD pattern of $Y_{2-x}O_3$:$Bi_{x=0.002}$ phosphor powder and the reference spectrum from the ICSD data base.

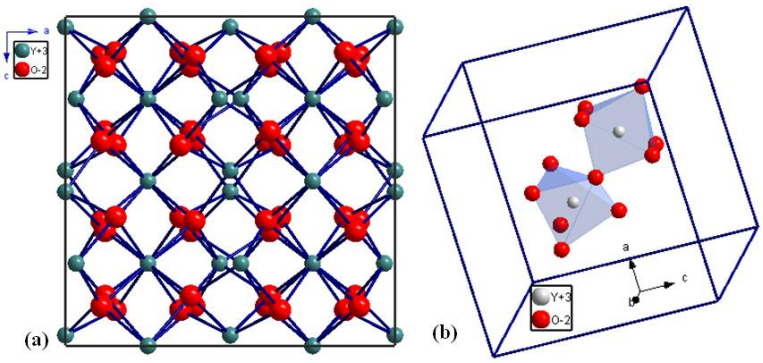

Figure 2: (a) The unit cell (ICSD-16394) and (b) schematic representation of the two different symmetry sites (S_6 and C_2) for the Y_2O_3 host.

3.2 Diffuse reflection spectra (DR) and band gap calculations

Figure (3) shows the diffuse reflectance measurements for Y_2O_3 and Y_2O_3:Bi samples against a reference standard ($BaSO_4$ compound). The band around 219 nm was observed for both the Y_2O_3 and Y_2O_3:Bi samples, which is attributed to the band gap as shown in Figure 3. The weak band around 280 nm was observed for the un-doped sample which is probably due to defect formation. The absorbance increased in the case of the Bi-doped sample and there are three bands, located around 255, 330 and 372 nm. These bands are due to the O^{2-}- Bi^{3+} charge transfer (CT) absorption to the different sites (C_2 and S_6 respectively).

The DR spectra for both the Y_2O_3 and Y_2O_3:Bi samples were used to calculate the band gap by using Kubelka-Munk and Tauc relation (1) [10], if the material scatters in a perfectly diffused manner.

$$F(R_\infty)^2 = C_1(h\nu - E_g) \qquad (1)$$

$R_\infty = R_{sample}/R_{reference}$ is the ratio of the light scattered from a thick layer of the sample and an ideal non-absorbing reference sample and it is measured as a function of the wavelength λ. E_g is the band gap, hυ is the photon energy and C_1 is a proportionality constant.

Plotting relation (1) as a function of $h\nu$, gives the value of the E_g by extrapolating the linear fitted regions to $[F(R_\infty)h\nu]^2 = 0$. The curve (as an inset in Figure 3) exhibits non-linear and linear portions, which are the characteristic of a direct allowed transition. The nonlinear portion corresponds to a residual absorption involving impurity states and the linear portion characterizes the fundamental absorption [10]. The calculated band gap was found to be almost 5.65 ± 0.1 eV for both Y_2O_3 and Y_2O_3:Bi samples which means that there is no change in the band gap when the Y_2O_3 host is doped with 0.2 mol % of Bi. Our results are in agreement with what Som et al. [10] have found. Their band gap was around 5.6 eV for Y_2O_3.

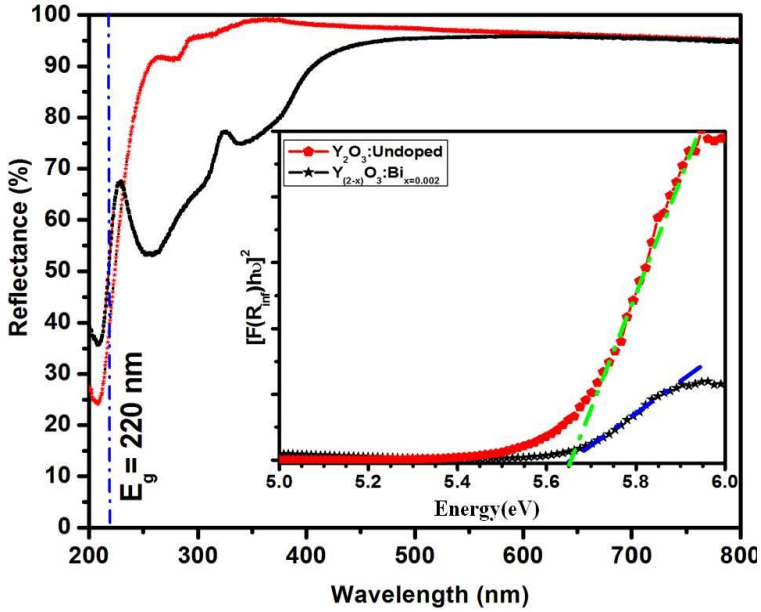

Figure 3: Diffuse reflection spectra measurements for Y_2O_3 and Y_2O_3:Bi samples.

3.3 Luminescence properties

Figure 4(a) shows the emission spectrum when the sample was excited with the 325 nm He-Cd laser. The phosphor has three emission bands, two bands centred at 360 nm and 407 nm (blue emission) and the other band is centred at 495 nm (green emission). Figure 4(b) shows the excitation and emission spectra of $Y_{2-x}O_3$:$Bi_{x=0.002}$ at room temperature. For emission at 495 nm (green emission) two excitation bands were observed in the 300 - 400 nm range, with maxima at 330 nm and 345 nm. For

emission at 407 nm (blue emission) two excitation bands were also observed in the 300 – 400 nm range but with maxima at 338 and 372 nm. For emission at 360 nm one excitation band centered at 345 nm were observed. When excited by 330 nm the same broad green emission with the two extra shoulders from the blue site was recorded. When excited by 372 nm the emission spectrum only showed a strong blue emission (407 nm) without any contribution from the green (495 nm) site [3,7,13-15]. The band centred at 330 nm is a result of the excitation of the Bi^{3+} ion in the C_2 site, where the band centered at 372 nm are a result of the excitation of the Bi^{3+} ion in the S_6 site [1,11,17]. There is a partial overlap between the 330, 338 and 345 nm excitation bands for the two different sites (C_2 and S_6) and this result in the two extra shoulders in the emission spectrum when excited by 330 nm radiation. If the phosphor is excited with 338 nm there is a slight increase in the blue emission bands (360 and 407 nm) and a slight decrease in the green emission band at 495 nm if compared to the emission spectra when excited by 330 nm. If the phosphor is excited with 345 nm there is an increase in 360 nm emission band and a decrease in the 407 and 495 nm emission bands.

The fact that the 325 nm HeCd laser and the excitation in the Cary Eclips Xe lamp between 300 to 400 nm show the same broad green emission spectrum indicates that the emission spectrum is not influenced by the excitation source. Figure 5 shows a schematic diagram of the energy levels in the free Bi^{3+} ion and of the Bi^{3+} ion in the C_2 and S_6 sites. The $^3P_1$ level is splitting into two (^3A_u and ^3E_u) and three (^3A, ^3B and ^3B) sub levels in the S_6 and C_2 symmetry sites respectively [11,16]. All the excitation bands are assigned to the $^1S_0 \rightarrow {}^3P_1$ transitions of the Bi^{3+} ion, in the multiple independent crystallographic cation sites, S_6 and C_2[1,7].

Figure 6 represent the chromaticity co-ordinates of the PL spectra for Y_2O_3:Bi, which were determined using the Commission Internationale de I'Eclairage (CIE) coordinates system. The algorithm is based on such intuitive color characteristics as tint, shade and tone. The coordinate system is cylindrical, and the colors are defined inside a hexcone. The algorithm also shows the position of the co-ordinates in the chromaticity diagram and the expected color of the material [17]. The calculated chromaticity coordinates for Bi^{3+} in the blue site (S_6) and the green site (C_2) are (0.16, 0.09) and (0.197, 0.320) respectively. It can be concluded that, two different chromaticity coordinates can be achieved from one luminescence center under different excitation bands.

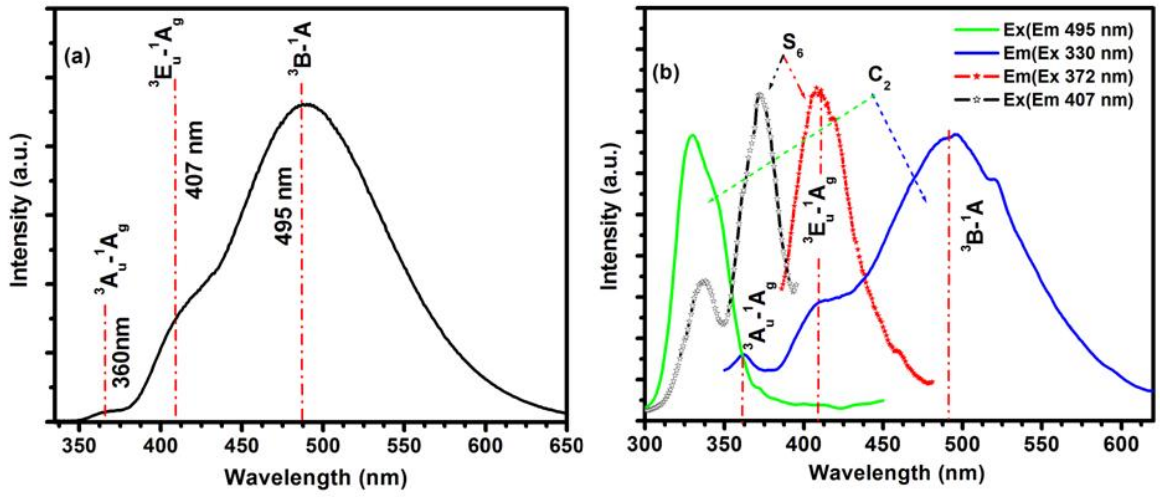

Figure 4: PL spectra of $Y_{2-x}O_3$:$Bi_{x=0.002}$ measured with (a) a 325 nm He-Cd laser and (b) with the Cary Eclipse Xe lamp.

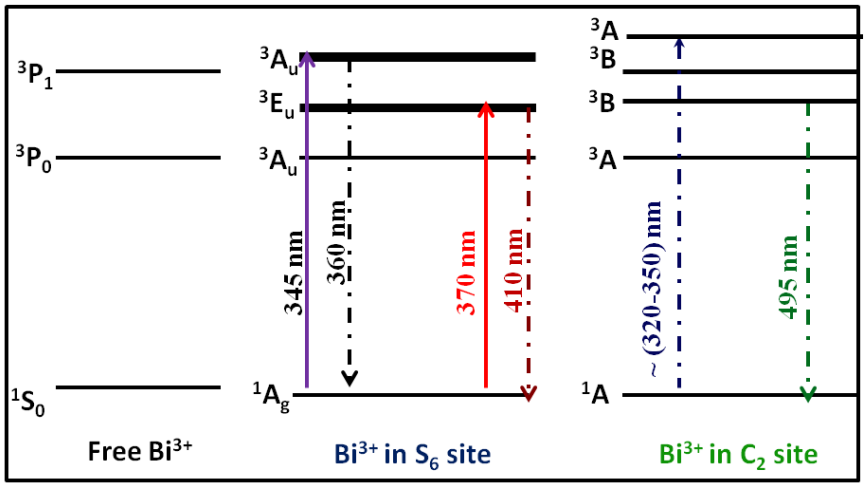

Figure 5: Schematic diagram of the energy levels of the Bi^{3+} ion [11].

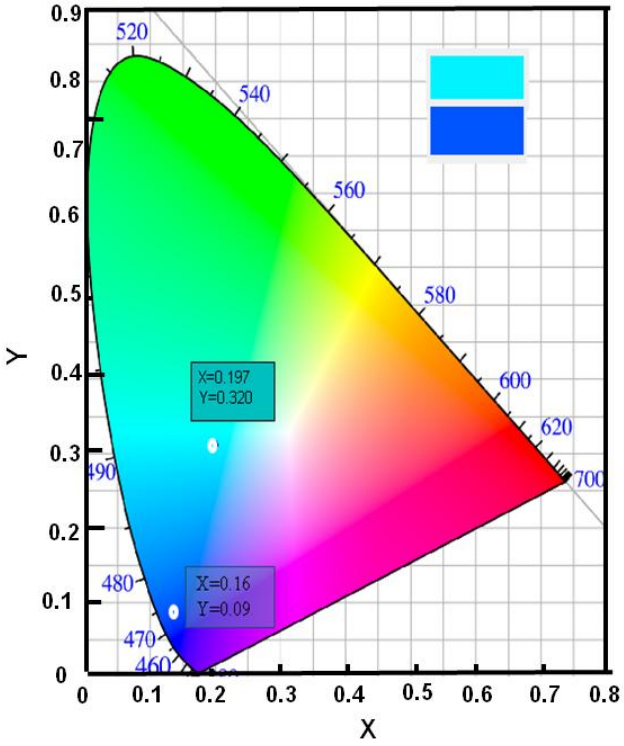

Figure 6: The calculated chromaticity coordinates for Bi^{3+} in the two different sites (S_6 and C_2)

4. Conclusion

The XRD results showed that the sample was successfully prepared by the combustion method and that the single cubic crystal structure phase with Ia-3 space group was formed. The DR spectra for the doped sample showed three bands located around 255, 330 and 372 nm. These bands are attributed to the O^{2-}- Bi^{3+} charge transfer (CT) absorption to the different sites (C_2 and S_6 respectively). The calculated band gap that was found to be almost 5.65 ± 0.1 eV for both the host and the doped sample indicated that the band gap is not affected by doping the host with Bi. The PL results showed that the phosphor have two emission bands centered at 360 and 407 nm for blue emission and a third band

centered at 495 nm for green emission. The excitation spectra showed 4 bands that corresponds to the $^1S_0 \rightarrow {}^3P_1$ transitions in the Bi^{3+} ion in the two different sites (S_6 and C_2). Excitation with the two main peaks at 330 and 372 nm result in broad green emission for the C_2 site and only blue emission for the S_6 site. Further investigations will be done with X-ray photo-electron spectroscopy to proof the two different sites that will contribute to the luminescent mechanism.

5. Acknowledgment

This work is based on the research supported by the South African Research Chairs Initiative of the Department of Science and Technology and National Research Foundation of South Africa. The University of the Free State Cluster program for financial support. We would like to thank Dr. R.E. Kroon for helping in the 325 nm He-Cd laser PL system.

References

[1] Huang X Y, Ji X H, Zhang Q Y 2011*American Ceramic Society* **94** 833

[2] Gorbenko V, krasnikov A, Mihokova E, Nikl M, Zazubovich S, Zorenko Yu 2013 ***J.****Luminescence* **134** 469

[3] Bordun O M, 2002 *Applied Spectroscopy* **69** 1

[4] Ju G, Hu Y, Chen L, Wang X, Mu Z, Wu H, Kang F 2011 *Electrochemical Society* **158** 294

[5] Huang X Y, Ji X H, Zhang Q Y 2011 *The American Ceramic Society* **94** 833

[6] Kumar V, Kumar R, Lochab S P, Singh N 2007 *Science Direct* **262** 194

[7] Jacobsohn L G, Blair M W, Tornga S C, Brown L O, Bennett B L 2008 *J. Applied Physics* **104** 124303.

[8] Schamps J, Flament J P, Real F, Noiret I 2003 *Optical Materials* **24** 221

[9] Babin V, Gorbenko V, Krasnikov A, Makhov A 2009 *J. Physics:Condensed Matter* **21** 415502

[10] Som S, Sharma S K 2012 *J. Physics D: Appied Physics*. **45** 415102

[11] Ju G, Hu Y,. Chen L, Wang X, Mu Z, Wu H, Kang F 2011 *J. The Electrochemical Society*. **158** 294

[12] Real F, Ordejon B, Vallet V, Flament J P, Schamps J 2009 *J. Chemical Physics* **131** 194501

[13] Chi L S, Liu R S, Lee B J 2005 *J. The Electrochemical Society* **152** 93

[14] Bordun O M 2002 *J. Applied Spectroscopy* **69**1

[15] Craats A M V D, Blasse G 1995 *Chemical Physics Letter* **234** 559

[16] Ju G, Hu Y, Chen L, Wang X, Mu Z,Wu H, Kang F 2012 *J. luminescence* **132** 1859

[17] Yousif A, Swart H C, Ntwaeaborwa O M 2013 *J. Luminescence* **143** 201

[18] Huang Z, Guo W, Liu Y, Huang Q, Tang F, Cao Y 2011 *Materials Chemistry and Physics* **128** 44

[19] Toma S Z,.Palumbo D T 1969 *J. Electrochemical Society*: Solid State Science**116** 2